THE ASTROPHYSICAL JOURNAL, 647:L37–L40, 2006 August 10

THEY CAME FROM THE DEEP IN THE SUPERNOVA: THE ORIGIN OF TiC AND METAL SUBGRAINS IN PRESOLAR GRAPHITE GRAINS

KATHARINA LODDERS
Planetary Chemistry Laboratory, Department of Earth and Planetary Sciences, and McDonnell Center for the Space Sciences, Washington University, Campus Box 1169, 1 Brookings Drive, St. Louis, MO 63130; lodders@wustl.edu
Received 2006 May 15; accepted 2006 June 27; published 2006 July 28

ABSTRACT

A new formation scenario for TiC and Fe-Ni metal inclusions in presolar graphite grains of supernova origin is described. The mineralogy and chemistry require condensation of Fe-Ni titanides from Fe-, Ni-, and Ti-rich gaseous ejecta, subsequent carburization to make TiC and metal, and encapsulation into graphite. Titanides only condense if Si is depleted relative to heavier elements, which requires α-rich freeze-out and a deep mass cut for the supernova ejecta. This Si-poor core material must remain unmixed with other supernova zones until the titanides condense. This can be accomplished by transport of core ejecta in bipolar jets through the major expanding supernova zone ejecta. If the jets stall in regions dominated by C-rich ejecta such as the C-He zone, where graphite condenses, thermochemically favored in situ carburization of the titanides—either before or during encapsulation into condensing graphite—leads to a TiC-and-metal composite. This scenario agrees with theoretical models and observations of asymmetric core collapse in supernovae that are associated with bipolar jets loaded with iron-peak elements.

Subject headings: astrochemistry — nuclear reactions, nucleosynthesis, abundances — supernovae: general — supernova remnants

1. INTRODUCTION

A small fraction of the known presolar graphite grains are thought to have originated in the ejecta of core-collapse, Type II supernovae (SNe II; see, e.g., reviews by Zinner 1998; Lodders & Amari 2005). These micron-size presolar graphite grains may contain 10–500 nm TiC and 10–80 nm kamacite (Fe-rich) metal subgrains (Croat et al. 2003, hereafter C03). The Fe-Ni metal subgrains are almost exclusively attached to TiC subgrains (only three out of 84 metal grains were not; see C03). Crystallographic evidence for epitaxial growth of Fe-Ni metal onto many TiC subgrains suggests the condensation sequence TiC–metal–graphite (C03).

However, it is not easy to only condense TiC, metal, and graphite in this order without any Si compounds. Usually, Si is as abundant as Fe (except in the innermost SN zones), so abundant Si compounds condense. However, SN II graphites *typically* do not contain internal SiC grains or other Si-rich phases. The graphite has only ~1% Si by weight (Hoppe et al. 1995; C03), TiC subgrains only have a ~0.05 atom fraction of Si on average, and Si is usually not detected in metal subgrains (C03). The low Si abundances rule out condensation of Si-bearing phases before TiC, metal, and graphite.

In contrast to the SN II graphites, presolar graphite grains from asymptotic giant branch (AGB) stars may contain TiC and refractory carbides of *s*-process elements, and typically, they have no metal or SiC subgrains (Bernatowicz et al. 1991, 1996). This agrees with the TiC–graphite–SiC–silicide condensation sequence in C-rich circumstellar shells of AGB stars with otherwise solar-like major-element composition (e.g., Lodders & Fegley 1995, 1999; Bernatowicz et al. 1996), but condensation from such a gas does not explain the SN II graphites with internal TiC and metal subgrains. However, elemental abundances in SN II ejecta are altered from solar by nucleosynthesis. The condensation sequences in different SN II zones are calculated in §§ 2 and 3. Condensation from any individual SN II zone cannot account for the observations. A condensation-reaction model for the TiC-metal-graphite grains is proposed in § 4. Section 5 briefly describes how asymmetric core-collapse SN II models and astronomical observations are consistent with the proposed condensation model, which is summarized in § 6.

2. CONDENSATES FROM SUPERNOVA ZONE COMPOSITIONS

Condensation calculations were done for averaged compositions of individual SN II zones from the 25 $M_\odot$ supernova model S25P by Rauscher et al. (2002, hereafter R02).[1] This more energetic model has 0.2 $M_\odot$ ^{56}Ni in the ejecta (twice that of their conventional 25 $M_\odot$ SN II model). This is more favorable for the required Ni- and Fe-rich chemistry of the presolar graphites with internal TiC and metal grains. Condensation results for conventional 15 and 25 $M_\odot$ SN II models by R02 are similar, but only results for model S25P are given here.

Calculations were performed with the CONDOR code (Lodders 2003). A nominal total pressure of $P_{tot} = 10^{-7}$ bars was adopted from the estimates by C03, but calculations were also done for different values of P_{tot}. The condensates for the different SN II zones are broadly similar to those reported by Lattimer et al. (1978) and Ebel & Grossman (2001), except that here silicides and titanides are included. Thermochemical properties for these are from Barin (1989), Knacke et al. (1991), and Kubaschewski (1983).

Compositions of the nominal SN II zones, named by their two most abundant elements, are listed in Table 1. The He-H, He-N, O-C, O-Ne, and O-Si zones with C/O < 1 yield condensates such as corundum, hibonite, perovskite, Mg silicates, and metal. Therefore, these zones are not considered further as contributors to the SN II graphites with subgrains.

The inner Si-S and Fe-Ni zones are very C- and O-poor (Table 1), and the condensates are silicides [Ti_5Si_3, (Fe,Ni)Si, $(Fe,Ni)_3Si$], sulfides, and metal (Table 2). Iron and nickel always co-condense, so it does not matter whether ^{56}Ni has de-

[1] See also http://www.ucolick.org/~alex/data.

TABLE 1
ADOPTED ATOMIC ZONE ABUNDANCES OF A 25 $M_\odot$ SUPERNOVA

Element	Fe-Ni Zone	Si-S Zone	O-Si Zone	O-Ne Zone	O-C Zone	C-He Zone	N-He Zone	He-H Zone
H	2.35×10^{2}	4.21×10^{-1}	5.60×10^{-2}	2.10×10^{1}	2.50×10^{1}	5.64×10^{-1}	5.06×10^{9}	2.03×10^{10}
He	1.09×10^{7}	9.00×10^{1}	4.00×10^{1}	5.68×10^{2}	3.79×10^{8}	9.28×10^{9}	8.44×10^{9}	4.63×10^{9}
C	3.50×10^{1}	1.11×10^{2}	2.20×10^{4}	2.80×10^{6}	6.94×10^{8}	4.38×10^{7}	1.02×10^{6}	3.09×10^{6}
N	9.80×10^{0}	6.78×10^{0}	1.37×10^{2}	4.19×10^{3}	3.20×10^{4}	3.10×10^{5}	3.38×10^{7}	2.10×10^{7}
O	1.90×10^{2}	2.68×10^{5}	6.81×10^{6}	1.04×10^{8}	1.42×10^{9}	3.21×10^{6}	2.18×10^{6}	1.29×10^{7}
Mg	8.20×10^{2}	5.88×10^{2}	1.99×10^{5}	6.21×10^{6}	2.77×10^{7}	1.23×10^{6}	1.06×10^{6}	1.07×10^{6}
Al	5.40×10^{2}	5.75×10^{2}	2.42×10^{4}	6.43×10^{5}	1.98×10^{5}	1.07×10^{5}	1.03×10^{5}	8.68×10^{4}
Si	1.00×10^{6}	1.00×10^{6}	1.00×10^{6}	1.00×10^{6}	1.00×10^{6}	1.00×10^{6}	1.00×10^{6}	1.00×10^{6}
S	7.96×10^{5}	4.62×10^{5}	2.70×10^{5}	3.05×10^{4}	2.48×10^{5}	4.84×10^{5}	5.15×10^{5}	5.15×10^{5}
Ca	2.60×10^{5}	4.49×10^{4}	9.19×10^{3}	1.12×10^{3}	1.88×10^{4}	5.46×10^{4}	6.11×10^{4}	6.11×10^{4}
Ti	1.49×10^{4}	3.67×10^{2}	2.60×10^{2}	4.10×10^{2}	4.66×10^{3}	2.36×10^{3}	2.40×10^{3}	2.40×10^{3}
Fe	9.62×10^{6}	7.69×10^{4}	1.15×10^{3}	1.49×10^{4}	2.70×10^{5}	8.60×10^{5}	9.00×10^{5}	9.00×10^{5}
Ni	5.90×10^{5}	2.52×10^{3}	2.02×10^{3}	2.53×10^{4}	3.68×10^{5}	4.81×10^{4}	4.94×10^{4}	4.94×10^{4}
C/O	1.80×10^{-1}	4.20×10^{-4}	3.20×10^{-3}	2.70×10^{-2}	4.90×10^{-1}	1.36×10^{1}	4.70×10^{-1}	2.40×10^{-1}

NOTE.—Scaled to Si = 10^6 atoms; only major elements are listed. Data from model S25P by R02.

cayed into ^{56}Fe or not. Graphite and TiC are not among the refractory condensates. The SN II graphites studied by C03 are Si-poor and without Si-rich subgrains, so the chemistry from the Si-S and Ni-Fe zones seems irrelevant.

Only the C-He zone, with high C/O, favors graphite formation, but condensation solely from this zone cannot explain the observation of graphite with internal TiC and metal. Graphite condenses several hundred kelvins higher than TiC at 10^{-7} bars (Table 2). Changes in P_{tot} by a few orders of magnitude do not alter this conclusion much, and it is difficult to reverse graphite and TiC condensation. If mixing of C-He zone material with material from its neighboring, O-rich zones occurs, the high C/O of ~13 that causes the high graphite condensation temperature can be reduced. Mixing of material from different zones is required to explain the C, N, and O isotopic compositions in presolar SN II graphites (see, e.g., Travaglio et al. 1999). As long as mixing gives C/O > 1, TiC and graphite can condense, and their condensation temperatures reverse at certain P_{tot}. But even if particular C/O ratios and total pressures lead to TiC condensation prior to graphite, there is condensation of $(Fe,Ni)_3Si$ (unobserved) instead of Fe-Ni metal (observed). This occurs whether mixing with neighboring zones reduces the original C/O. Also, SiC condenses prior to silicide in the C-He zone. The observed TiC–metal–graphite condensation sequence is incompatible with the calculated sequence graphite–TiC–SiC–$(Fe,Ni)_3Si$ for the C-He zone, or TiC–graphite–SiC–$(Fe,Ni)_3Si$ for the C-He zone with admixtures from the O-C zone, He-N zone, or both.

TABLE 2
CONDENSATES AND CONDENSATION TEMPERATURES

Condensate	Fe-Ni Zone	Si-S Zone	C-He Zone
C	...	...	2055
TiC	...	...	1579
SiC	...	...	1405
Ti_5Si_3	1622	1641	...
TiSi	...	1609	...
(Fe, Ni)Si	1528	1546	...
$(Fe, Ni)_3Si$	1461	...	1176
Fe, Ni	1434	...	...
Si	...	1507	...
CaS	1398	1262	1099

NOTE.—At 10^{-7} bars and the averaged zone compositions in Table 1 (in kelvins).

None of the zone-averaged SN II compositions gives the condensation sequence TiC–metal–graphite implied by the observations. However, presolar SN II graphite grains also contain decay products of ^{44}Ti ($t_{1/2}$ = 58 yr) and ^{49}V ($t_{1/2}$ = 337 days), and their production is expected only in the innermost SN II zones (Nittler et al. 1996; Hoppe & Besmehn 2002). As the grains do not contain much Si, Si-poor compositions are needed. All this leads us to dig deeper into the Fe-Ni core.

3. CONDENSATES FROM Si- AND S-POOR Ni-Fe ZONE COMPOSITIONS

I now consider the effect of compositional gradients across the Ni-Fe zone. Figure 1 (*top*) shows the mass fractions of Fe, Ni, Ti, Si, Ca, and S as a function of interior SN II mass from the S25P model by R02. The Ni-Fe zone composition depends on the energy of the reverse shock, mass cut, and fallback from the SN II explosion. The border between the Si-S and the Ni-Fe zones is taken where the mass fraction of Fe (after ^{56}Ni decay) is larger than that of Si. From this border inward, Fe and Ni abundances increase to constant high values, whereas Si, S, and Ca abundances significantly drop, go through a minimum, and level out to constant low values. The Ti abundance increases less steeply than that of Fe and Ni and moves through a minimum like Si, Ca, and S before leveling out. The steep changes over orders of magnitude show that the Ca, Si, and S abundances of the averaged Ni-Fe zone in Table 1 are mainly given by Ni-Fe zone layers near the Si-S zone. Only deep in the Ni-Fe zone are Fe, Ni, and Ti much more abundant than Si.

The bottom panel of Figure 1 shows the condensation chemistry along the mass profile shown in the panel above. Compositions near the Si-S zone give the same condensates [Ti_5Si_3, (Fe,Ni)Si, $(Fe,Ni)_3Si$, Fe-Ni metal, and CaS] as in the average Ni-Fe zone (Table 2). But deeper, the titanide $(Fe,Ni)_2Ti$ condenses instead of the silicides because Si abundances are minimized. After the Si minimum is passed, initial condensates are Ti_5Si_3, $(Fe,Ni)_2Ti$, and Fe-Ni. Condensation of $(Fe,Ni)_2Ti$ is the key to the presolar grain observations (§ 4), but it is not the first condensate for the compositions in Figure 1 (*top*), and CaS or Ti_5Si_3—neither observed in the presolar graphites—condenses first (Fig. 1, *bottom*). Although the Ni-Fe zone in the S25P model by R02 is already more Fe- and Ni-rich than in their conventional models, there still is abundant S, Si, and Ca from incomplete Si burning. This changes under very en-

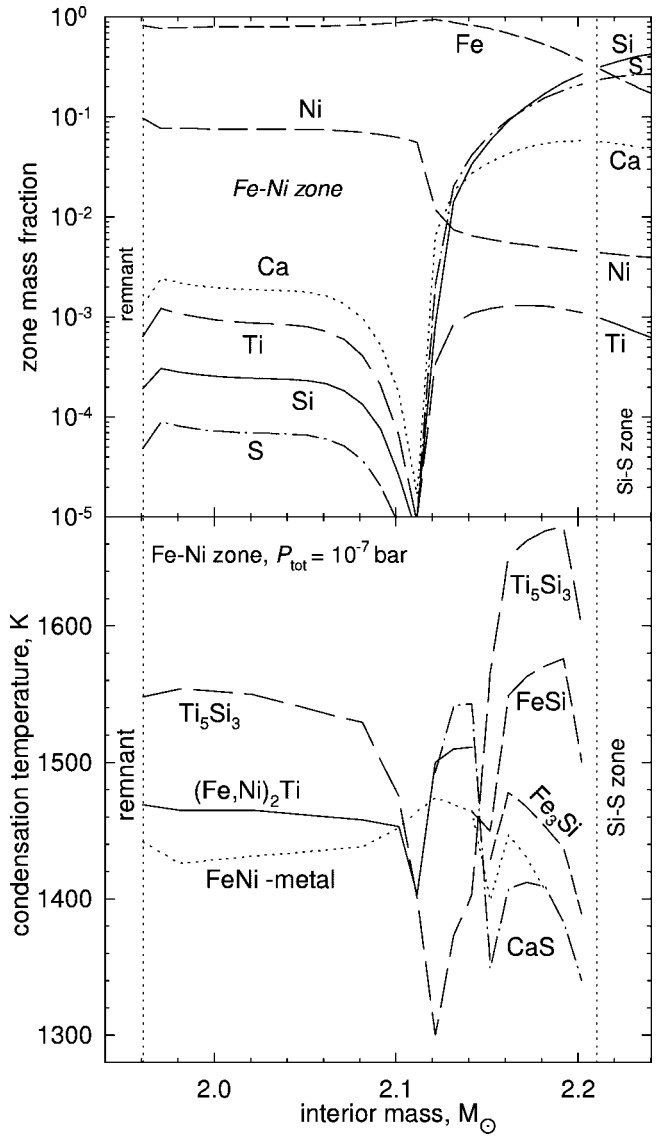

FIG. 1.—*Top*: Ni-Fe zone composition along the interior mass for the 25 $M_\odot$ SN II model S25P by R02. Vertical lines indicate borders of the stellar remnant and the neighboring Si-S zone. *Bottom*: Condensates and condensation temperatures at $P_{tot} = 10^{-7}$ bars for the compositions shown above. At $M < 2.1\ M_\odot$, CaS condensation temperatures are below 1300 K because Ca and S abundances drop.

ergetic conditions, in which complete Si burning with α-rich freeze-out leaves heavy Fe-peak nuclides (including ^{44}Ti) and significantly reduces Si, S, and other lighter Z elements, which is required in order to explain the observed chemistry.

Figure 2 shows the changes when Si and S abundances in the nominal Ni-Fe zone composition (Table 1) are decreased by the same factor. The nominal composition gives Ti_5Si_3, (Fe,Ni)Si [which transforms into $(Fe,Ni)_3Si$ at lower temperatures], and Fe-Ni metal. With decreasing Si and S content, metal condensation temperatures are unchanged, but those of the silicides drop dramatically. The Fe- and Ni-bearing silicides are replaced by $(Fe,Ni)_2Ti$ when Si and S abundances are ~4% of their nominal values. The $(Fe,Ni)_2Ti$ condensation temperature increases with further Si and S reductions. Decreasing the Si and S abundances by more than a factor of 1000 only leaves $(Fe,Ni)_2Ti$ and Fe-Ni metal.

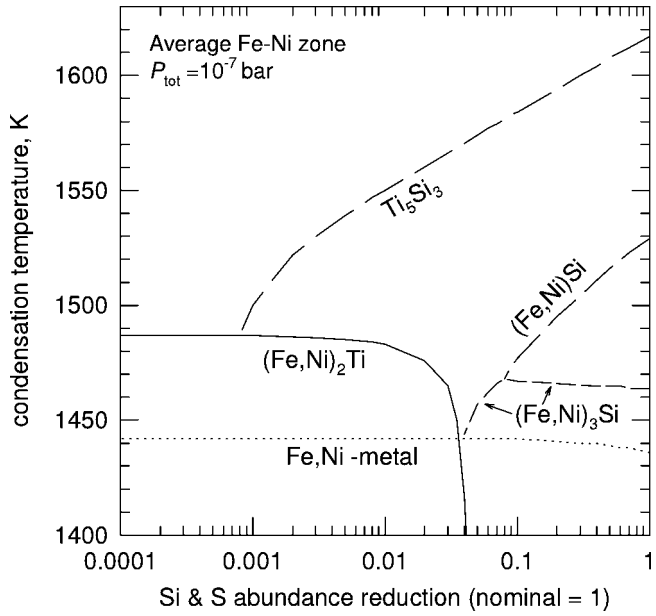

FIG. 2.—Effect on condensates of reducing Si and S abundances by the same factor from the nominal Ni-Fe zone composition (Table 1). The CaS condensation temperatures (not shown) decrease from ~1400 K at the nominal composition with decreasing S abundances.

4. FORMATION OF THE TiC-METAL COMPOSITES

Condensation of $(Fe,Ni)_2Ti$ [and/or (Fe,Ni)Ti, depending on the details of P_{tot} and compositions] from Ni-Fe zone ejecta opens a new route to make the TiC and metal subgrains in presolar graphites. Consider an Fe-Ni titanide that condensed from Ni-Fe zone ejecta and reached the C-rich C-He zone. There, thermochemically favored in situ carburization of the titanide gives a TiC-metal composite:

$$(Fe,Ni)_nTi + C = TiC + n(Fe,Ni). \quad (1)$$

This reaction may happen before or during encapsulation of the particles into graphite as it condenses, and it fits the observations by C03 that almost every metal subgrain is attached to a TiC subgrain in the graphites. Depending on temperature, titanides and metal are either solid or liquid (melting points 1427°C [Fe_2Ti], 1570°C [FeTi], and 1538°C [Fe]), whereas TiC (mp 3067°C) is solid. Liquids can facilitate diffusion of C to form TiC from the titanides. The observed crystallographic alignments of TiC and metal surfaces in the presolar graphite grains may result from reordering in the solid (or liquid) phase during in situ carburization, instead of the epitaxial growth (i.e., metal vapor deposition onto TiC) suggested by C03. However, this requires more investigation.

In situ titanide carburization is consistent with the observed diameters of the TiC-metal assemblages in the presolar graphites. The TiC grain diameters typically are larger than those of their attached metal grains, and TiC : metal diameter ratios in the sliced graphite grains range from ~2 to ~6 (C03). If metal were freely condensing onto TiC, one would expect much thicker metal layers than TiC diameters because Fe and Ni abundances, and thus the condensable metal volume, are generally much larger than that of Ti in any SN II zone.

It is easy to compare expected TiC : metal diameter ratios with the presolar-grain observations. In reaction (1), TiC and Fe-Ni metal form in molar proportions of 1 : 2 from $(Fe,Ni)_2Ti$

($n = 2$) or 1:1 from (Fe,Ni)Ti ($n = 1$). Using densities of $\rho_{Fe} = 7.87\ cm^3\ g^{-1}$ and $\rho_{TiC} = 4.93\ cm^3\ g^{-1}$, the molar volume ratio is $V_{TiC}/V_{met} = 0.86$ for $n = 2$ (1.7 for $n = 1$). The Ni content in the metal is neglected for simplicity. Using denser Fe-Ni alloys slightly increases the TiC : metal diameter ratios. If the assemblage consists of a TiC sphere next to a metal sphere, the diameter ratio is $a_{TiC}/a_{met} = 0.95$ for $n = 2$ (1.2 for $n = 1$). The metal thickness (x_{met}) on *one* side of a solid TiC sphere evenly coated by metal (as seen when the sphere is sliced) relative to the TiC diameter is $a_{TiC}/x_{met} = 6.8$ for $n = 2$ (12 for $n = 1$). The calculated TiC : metal diameter ratios of ~1 to ~7 from $(Fe,Ni)_2Ti$ carburization are similar to the observed ratios of ~2 to ~6. This suggests condensation and subsequent carburization of $(Fe,Ni)_2Ti$ instead of TiC and metal condensation from a gas enriched in Fe and Ni.

5. SUPERNOVA SETTING

The proposed formation process of internal TiC and metal grains in presolar SN II graphite requires

1. Complete α freeze-out near the SN II core to make Fe-, Ni-, and Ti-rich but Si- and S-poor ejecta;
2. Transport of Ni-Fe zone ejecta across the Si-S, O-Si, O-Ne, and O-C zones without mixing so that Fe-Ni titanides condense; and
3. Carburization of the titanide in the C-He zone.

These conditions can be realized by jet-driven, nonspherical core-collapse supernovae.

Khokhlov et al. (1999) showed that magnetorotationally induced supersonic jets in the core of a massive star cause nonspherical SN explosions in which most of the material is expelled in oblate, distorted ejecta and a smaller amount is ejected in high-velocity bipolar jets. Nagataki et al. (1997) and Nagataki (2000) showed that jetlike explosions cause active α-rich freeze-out behind the more energetic shock wave in the polar regions, and that the high-velocity jets launched from the poles are very likely rich in Fe-peak elements. Hence, bipolar jets from asymmetric core collapse provide the nucleosynthesic setting for α-rich freeze-out and the transport of Fe-, Ni-, and Ti-rich ejecta to the C-He zone to make the observed TiC-metal composites in the presolar graphites.

Nonspherical explosion models with associated jets can account for many observations in SNe and their remnants (e.g., SN 1987A, Cas A, Vela) for which conventional spherical models fail (see, e.g., Nagataki et al. 1997; Nagataki 2000; Khokhlov et al. 1999; Höflich et al. 2002; Hungerford et al. 2003). For example, double-peaked SN light curves fired by ^{56}Ni-containing ejecta moving at different velocities and asymmetric features in supernova remnants are most plausibly due to high-velocity bipolar jets that cause ^{56}Ni-rich (later Fe-rich) "bullets," "clumps," and "knots" in the outer ejecta zones (see, e.g., Wang et al. 2002; Hwang & Laming 2003; Willingale et al. 2003; Tominaga et al. 2005). Wang et al. (2002) concluded that the observed bipolar structure of SN 1987A and the high-velocity ejecta rich in ^{56}Ni are best explained by assuming that nonrelativistic jets drove the SN explosion and led to ^{56}Ni- and ^{44}Ti-rich plumes being ejected along the jet axis to the overall expanding ejecta. It seems that many SN observations almost directly probe the necessary conditions to make the TiC-metal composites in the presolar graphites.

6. SUMMARY

Presolar SN II graphite with composite TiC-metal subgrains cannot be formed from any single SN II zone composition, such as the C-rich C-He zone, or by considering moderate mixing of the C-He zone with its neighboring He-N and O-C zones. The formation of TiC-metal composites requires complete Si burning with α-rich freeze-out to obtain ejecta from which $(Fe,Ni)_2Ti$ can condense. Jet-driven, axisymmetric core collapse can lead to α-rich freeze-out in the polar regions at the Ni core and create bipolar jets carrying ejecta rich in Fe-peak elements (e.g., Nagataki et al. 1997; Khokhlov et al. 1999). Condensation of $(Fe,Ni)_2Ti$ must occur in the chemical environment of the jets that pass through the main ejecta. If the jets stall in the C-rich C-He zone, carburization of the titanide to the TiC-metal composite takes place either before or during encapsulation of the TiC-metal composite into graphite.

I thank T. Bernatowicz and K. Croat for discussions about presolar grains, and B. Fegley and S. Woosley for comments on the manuscript. Careful comments by referee R. Gallino are much appreciated. This work was supported in part by NASA grant NNG04GG13G.

REFERENCES

Barin, I. 1989, Thermochemical Data of Pure Substances (Weinheim: VCH)
Bernatowicz, T. J., Amari, S., Zinner, E. K., & Lewis, R. S. 1991, ApJ, 373, L73
Bernatowicz, T. J., Cowsik, R., Gibbons, P. C., Lodders, K., Fegley, B., Jr., Amari, S., & Lewis, R. S. 1996, ApJ, 472, 760
Croat, T. K., Bernatowicz, T. Amari, S., Messenger, S., & Stadermann, F. J. 2003, Geochim. Cosmochim. Acta, 67, 4705 (C03)
Ebel, D. S., & Grossman, L. 2001, Geochim. Cosmochim. Acta, 65, 469
Höflich, P. A., Baade, D., Khokhlov, A. M., Wang, L., & Wheeler, J. C. 2002, in IAU Symp. 212, A Massive Star Odyssey, ed. K. van der Hucht, A. Herrero, & C. Esteban (San Francisco: ASP), 387
Hoppe, P., Amari, S., Zinner, E., & Lewis, R. S. 1995, Geochim. Cosmochim. Acta, 59, 4029
Hoppe, P., & Besmehn, A. 2002, ApJ, 576, L69
Hungerford, A. L., Fryer, C. L., & Warren, M. S. 2003, ApJ, 594, 390
Hwang, U., & Laming, J. M. 2003, ApJ, 597, 362
Khokhlov, A. M., Höflich, P. A., Oran, E. S., Wheeler, J. C., Wang, L., & Chtchelkanova, A. Yu. 1999, ApJ, 524, L107
Knacke, O., Kubaschewski, O., & Hesselmann, K., eds. 1991, Thermochemical Properties of Inorganic Substances (2nd ed.; Berlin: Springer)
Kubaschewski, O. 1983, in Titanium: Physico-Chemical Properties of Its Compounds and Alloys, ed. K. L. Komarek (At. Energy Rev. Spec. Issue 9) (Vienna: Int. At. Energy Agency), 3
Lattimer, J. M., Schramm, D. N., & Grossman, L. 1978, ApJ, 219, 230
Lodders, K. 2003, ApJ, 591, 1220
Lodders, K., & Amari, S. 2005, Chem. Erde, 65, 93
Lodders, K., & Fegley, B., Jr. 1995, Meteoritics, 30, 661
———. 1999, in IAU Symp. 191, Asymptotic Giant Branch Stars, ed. T. Le Bertre, A. Lèbre, & C. Waelkens (San Francisco: ASP), 279
Nagataki, S. 2000, ApJS, 127, 141
Nagataki, S., Hashimoto, M.-A., Sato, K., & Yamada, S. 1997, ApJ, 486, 1026
Nittler, L. R., Amari, S., Zinner, E., Woosley, S. E., & Lewis, R. S. 1996, ApJ, 462, L31
Rauscher, T., Heger, A., Hoffman, R. D., & Woosley, S. E. 2002, ApJ, 576, 323 (R02)
Tominaga, N., et al. 2005, ApJ, 633, L97
Travaglio, C., Gallino, R., Amari, S., Zinner, E., Woosley, S., & Lewis, R. S. 1999, ApJ, 510, 325
Wang, L., et al. 2002, ApJ, 579, 671
Willingale, R., Bleeker, J. A. M., van der Heyden, K. J., & Kaastra, J. S. 2003, A&A, 398, 1021
Zinner, E. 1998, Annu. Rev. Earth Planet. Sci., 26, 147